Selective growth of horizontally-oriented carbon nanotube bridges on patterned silicon wafers by electroless plating Ni catalysts

Chen-Chun Lin, Po-Lin Chen, Chi-Ting Lin, Cheng-Tzu Kuo *

Institute of Materials Science and Engineering, National Chiao Tung University, 1001 Ta-Hsueh Road, Hsinchu 300, Taiwan

Available online 28 September 2005

Abstract

The main purpose of this research was to develop an Integrated Circuit compatible process to grow the horizontally-oriented carbon nanotubes (CNTs) across the trenches of the patterned Si wafer, which was produced by conventional photolithography technique. The selectivity of the process is based on the difference in electrical conductivity between amorphous silicon (a:Si) and silicon nitride (Si_3N_4), where the catalyst can be much easier deposited by electroless plating on the a:Si part of the pattern. The selectivity is also based on greater chemical reactivity of the catalyst with a:Si to form silicides, instead of with Si_3N_4. Furthermore, the Si_3N_4 barrier layer of the pattern was designed on top of the a:Si layer to guide the growth of CNTs in horizontal direction to bridge the trenches of the pattern. The as-deposited catalysts were examined by Auger electron spectroscopy (AES). The catalyst-coated pattern was pretreated in hydrogen plasma and followed by CNT growth in a microwave plasma chemical vapor deposition (MPCVD) system. The CNT bridges were characterized by scanning electron microscopy (SEM), transmission electron microscopy (TEM), high-resolution TEM (HRTEM), and I–V measurements. Under the present deposition conditions, TEM and HRTEM examinations indicate that the deposited nanostructures are bamboo-like multiwalled carbon nanotubes (MWNTs) with a wall thickness of 20~30 graphene layers. Electrical conductivity of the as-deposited MWNTs can be greatly improved by subjecting to 760 °C heat treatment under nitrogen atmosphere. The results demonstrate that the amounts of CNTs and bridges are tunable with the Ni catalyst plating time. Under the present experimental configuration and at a catalyst plating time of 20 s, countable numbers of bridges can be obtained, which are selectively and horizontally grown on the areas of the pattern with Ni catalyst. This process can be a step approaching the application of CNTs in electronic devices.
© 2005 Elsevier B.V. All rights reserved.

Keywords: Carbon nanotubes (CNTs); Electroless plating; Selective deposition process; Microwave plasma chemical vapor deposition (MPCVD)

1. Introduction

Carbon nanotubes (CNTs) are novel carbon materials with unique electrical and mechanical properties [1–4]. They can be considered as a result of folding graphite layers into carbon cylinders and may be composed of a single shell for single-walled nanotubes (SWNTs), or of several shells for multi-walled nanotubes (MWNTs). The CNTs can behave metallic or semiconducting properties, depending on their rolling helicity or chirality [5,6]. Because of their unique electrical properties and nanoscale dimensions, CNTs are good candidates for nanoscale electronic devices.

Experiments over the past several years have been conducted to fabricate the functional nano devices with CNTs and to incorporate into electronic circuits that hopefully work far more faster than and less power consumption than existing electronic devices. For example, CNTs have been used as circuit components to be modulated to generate carbon nanotube field-effect transistors (CNT-FETs) [7–10]. However, until now the industrial application of CNTs for electronic devices has not been realized because of difficulty in the assembly and integration with the well-established silicon IC technology. Therefore, it would be desirable from both scientific and technological points of view to control not only the size and chirality of CNTs, but also their position and orientation.

* Corresponding author. Tel.: +886 3 5731949; fax: +886 3 5721065.
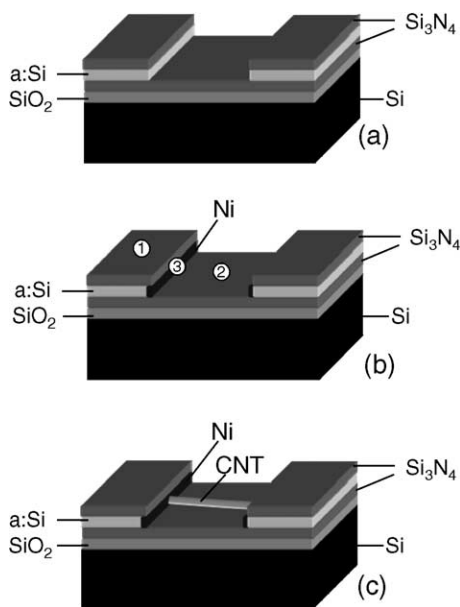 *E-mail address:* ctkuo@mail.nctu.edu.tw (C.-T. Kuo).

Fig. 1. Schematic diagrams showing the catalyst and CNTs deposition locations and procedures on trench of the pattern.

In this paper, we plan to synthesize directly the floated CNT bridges on silicon wafers that were patterned though conventional photolithography of the silicon semiconductor processes.

2. Experimental

A process was designed to grow the horizontally-oriented CNTs across the trenches of the patterned Si wafer, which was produced by conventional photolithography technique. The process is schematically shown in Fig. 1. At first, a 100 nm-thick SiO_2 layer, a 100 nm-thick Si_3N_4 layer, a 50 nm-thick a:Si layer, and a 100 nm-thick Si_3N_4 layer were grown orderly on Si wafer by Low Pressure- Chemical Vapor Deposition (LP-CVD). The 400 nm-wide trenches on the wafer were then created by Reactive Ion Etching (RIE) process (Fig. 1(a)). The second step was to selectively deposit the Ni catalyst for CNTs growth onto the side wall of a:Si layer by electroless plating, where the catalyst could preferentially be deposited on a:Si areas due to a greater electrical conductivity of a:Si than Si_3N_4 (Fig. 1(b)). The selectivity is also based on greater chemical reactivity of the catalyst with a:Si to form silicides, instead of with Si_3N_4. The electroless solution was made by mixing the solutions of 10 ml 10% N_2H_4, 0.5 g 0.02 M $NiSO_4$•6 H_2O, 0.5 g 0.1 M NH_4Cl, 20 ml 1.4% NH_4OH and 140 ml de-ionized water at 100 °C. The selectively deposited Ni catalyst pattern was then pretreated in H plasma ($H_2 = 100$ sccm, 400 W, 9 Torr, and 550~580 °C) in the MPCVD system. It was then followed by CNTs deposition with Ni as catalyst and CH_4 and H_2 as source gases (Fig. 1(c)). The CNTs deposition conditions are $CH_4/H_2 = 1/100$ sccm/sccm, 800 W microwave power, under 16 Torr and 660~680 °C. It is worth to

mention that the Si_3N_4 barrier layer of the pattern was designed on top of the a:Si layer to guide the growth of CNTs in horizontal direction to bridge the trenches of the pattern.

The distribution and chemical bonding of the as-deposited catalysts were examined by Auger electron spectroscopy (AES). The morphologies and microstructures of CNT bridges were characterized by scanning electron microscopy (SEM), transmission electron microscopy (TEM) and high-resolution TEM (HRTEM). The electrical properties of the as-deposited and the annealed (at 760 °C) CNTs were evaluated by I–V measurements (HP4156).

3. Results and discussion

3.1. Morphologies and lattice images of the catalyst nanoparticles and CNTs

In order to develop the CNTs deposition conditions, the Ni catalyst film were deposited on the Si wafer by electroless plating and then followed by H-plasma pretreatment to form the well-distributed Ni nanoparticles. The SEM morphology of Ni catalyst nanoparticles with a number density around 100 particles/μm^2 is shown in Fig. 2(a). The corresponding
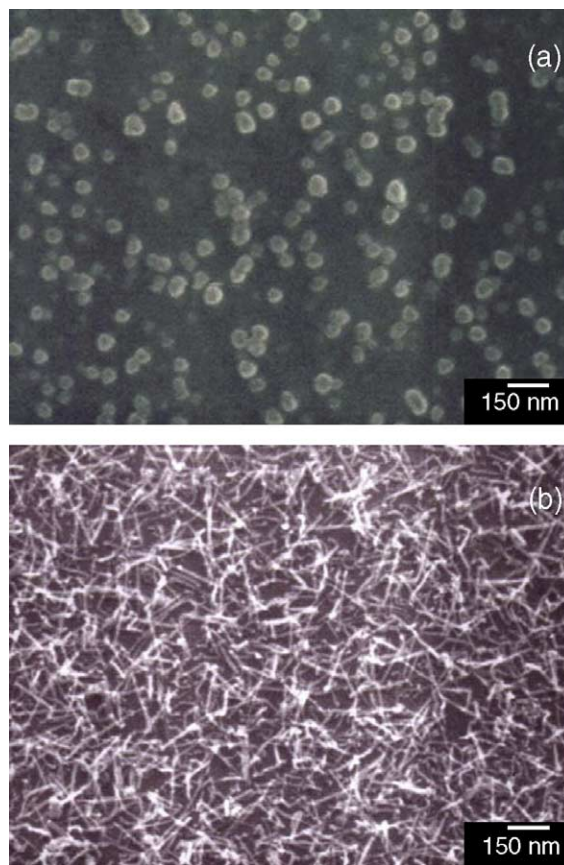

Fig. 2. SEM micrographs of, (a) the H-plasma-pretreated Ni catalyst particles, and (b) the as-deposited Ni-assisted CNTs on Si wafers, respectively.
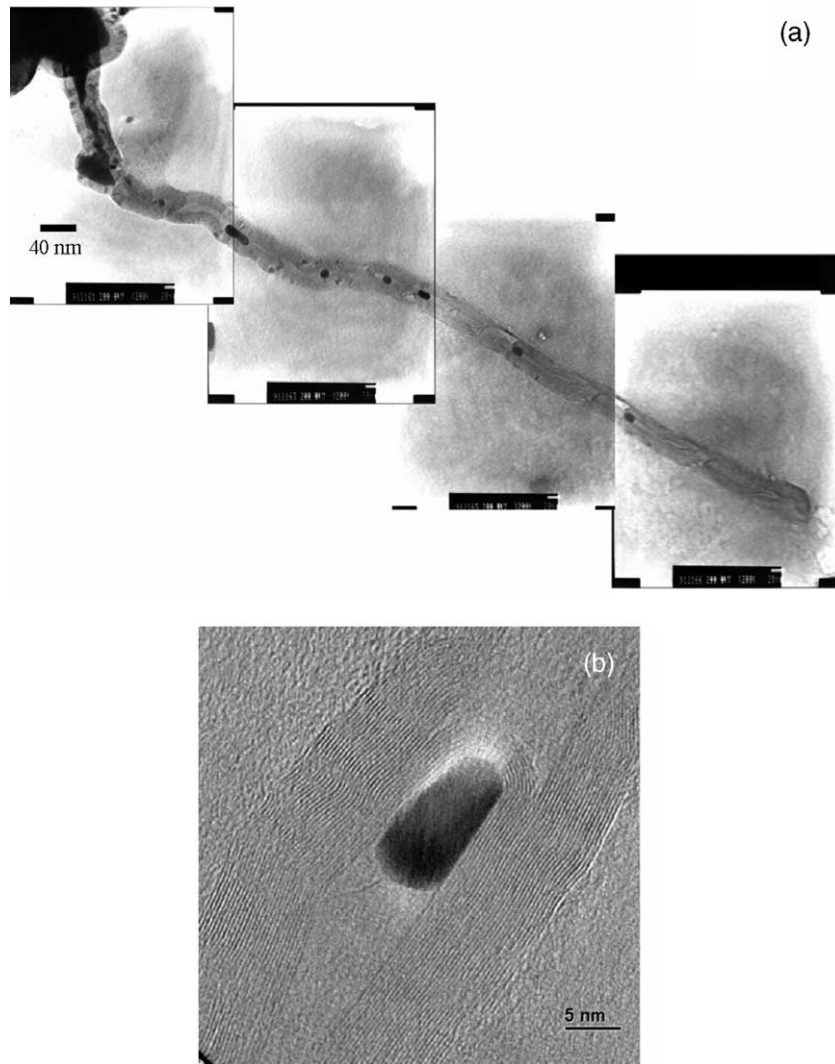
Fig. 3. (a) TEM micrograph showing morphology of the as-deposited bamboo-like CNTs with discrete catalyst particles split from one original particle in the tube, and (b) the corresponding HRTEM lattice image of a compartment of the tube around the split catalyst.

SEM micrograph of the as-deposited Ni-assisted CNTs is depicted in Fig. 2(b), where the typical features of the CNTs are 100~1200 nm in length, 10~30 nm in diameter, and 2000 tubes/μm^2 (=1290 Gtubes/inch^2) in tube number density. In other words, in average, there are about 20 nanotubes grown on each catalyst, and directions of the

CNTs were randomly oriented. In this case, the electroless plating time of Ni was 40 s.

Fig. 3(a) is the TEM image of an as-grown CNT, depicting a root-growth bamboo-like MWNT with discrete catalyst particles (about 5~15 nm in size) split from one original particle in the tube. It is interesting to note that the
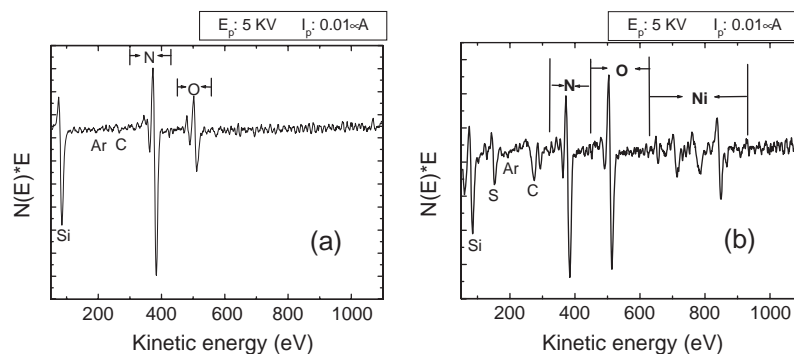

Fig. 4. Auger spectra at, (a) Positions 1, 2, and (b) Position 3 in Fig. 1(b) on the pattern after Ni catalyst deposition.

bamboo-like MWNTs synthesized without introducing N_2 during CNTs deposition seem to be contradictory to the proposed mechanism in the literature [11]. The possible reason may be due to the residual nitrogen on specimen during electroless catalyst deposition, as indicated in Auger analysis in the next paragraph for the as-deposited Ni film. HRTEM lattice image around a compartment of bamboo-like CNTs is shown in Fig. 3(b). The tube wall is composed of about 20~30 layers of graphene sheets, and widthwise side of the compartment consists of 10~15 graphene sheets.

3.2. Auger spectra of the Ni catalyst-deposited pattern

In order to investigate the composition and distribution of the as-deposited catalyst pattern, the Ni-patterned Si wafer was examined by AES at Positions 1, 2 and 3 in Fig. 1(b) after Ni electroless plating for 40 s. The AES spectra for Position 1 (at the top Si_3N_4 layer) and Position 2 (at the bottom of the trench) are almost the same and the typical one is shown in Fig. 4(a). It indicates Si and N peaks from Si_3N_4 layer, C and O peaks from surface absorptions, and S peak from residual electroless solution $NiSO_4 \cdot 6H_2O$. In contrast, we can only detect the Ni peaks at the side wall of the a:Si layer, as shown in Fig. 4(b) for Position 3 in Fig. 1(b). In other words, the Ni catalysts were successfully selectively deposited on the a:Si layers of the pattern.

3.3. Morphologies of the Ni-assisted MWNTs on the pattern

The results indicate that the plating time is a crucial parameter to manipulate the tube number density of MWNTs. For Ni plating time of 10 s, the catalyst was merely deposited on the corner of the trench and the CNTs started to grow at the corner. For Ni plating time of 15 s (Fig. 5(a)), the CNTs were grown from the catalyst film on the trench wall. Further increases in plating time to 20 s, the CNTs grown on the Ni pattern are long enough to cross the trench due to flow guidance of Si_3N_4 layer on top of Ni layer, as shown in Fig. 5(b). Furthermore, while the electroless plating time of Ni is over 30 s (Fig. 5(c)), the trench would be filled by the randomly oriented CNTs due to mutual restrictions from the neighboring CNTs.

The typical CNTs bridge in Fig. 5(b) is conformed to our previous work to synthesize the well-aligned horizontally-oriented CNTs on Si wafer under −200 V substrate bias and by using ECR-CVD, where the source gases were guided to flow horizontally by a Ti foil positioned 1~2 mm on top of the specimen [12]. Similar process was reported by Han, et al. [10]. They control the diameter, tube number density and orientation of CNTs on the pattern by varying the catalyst thickness, pressure, acetylene gas concentration and temperature. The horizontally-aligned CNTs bridges were also prepared on the patterned Si towers with no catalysts on the pattern by thermal CVD, where the source gases were guided to flow through the catalyst bed [13], and prepared on a poly-Si pattern by the electric field-assisted thermal
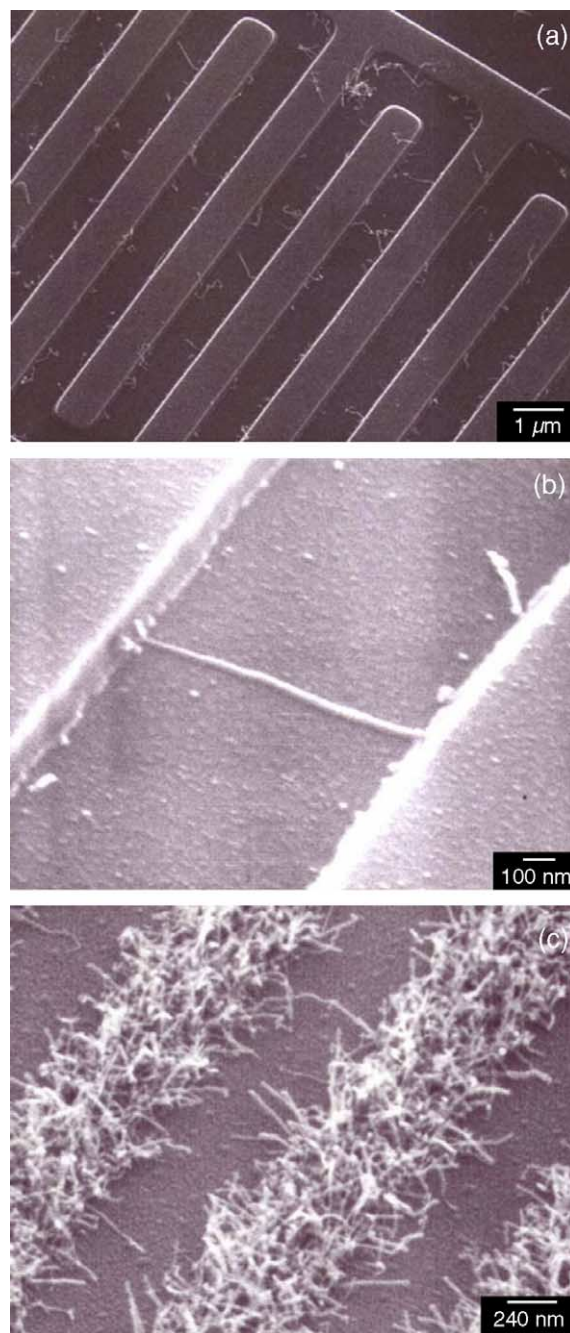

Fig. 5. SEM micrographs of the as-deposited CNTs on Ni-coated patterns under different catalyst electroless plating times, (a) 15, (b) 20, and (c) 60 s, respectively.

CVD [14]. The growth mechanisms of these CNTs bridges are still a controversy issue. The proposed mechanisms are based on the following arguments: growth competition due to interaction between flow rate and flow direction differences plus van der Waals interaction [15,16]; growth directed by interaction between electric field and the CNTs [13], where the field-alignment effect originates from the high polarization ability of CNTs. We propose that the physical restriction of Si_3N_4 layer on top of Ni catalyst layer and the self-generated electric potential difference between
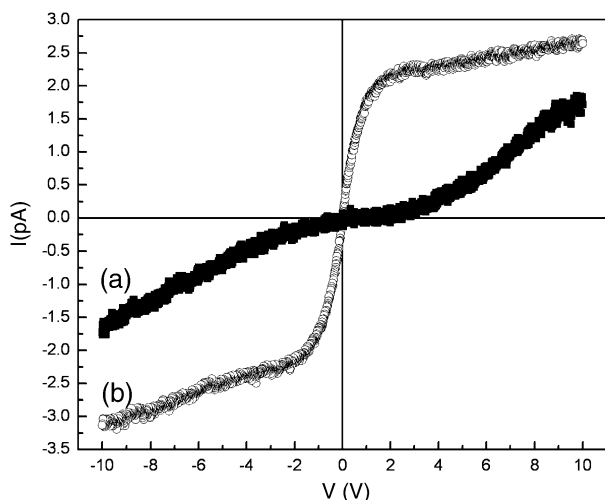
Fig. 6. The I–V curves for, (a) the as-deposited, and (b) the annealed horizontally-oriented CNTs patterns, respectively.

the trench walls will guide the ions to flow horizontally, and the tube number density can be controlled through manipulating the catalyst plating time to minimize the mutual growth restrictions by the neighboring tubes; so the CNTs can be grown horizontally to form bridges between trenches.

3.4. The I–V curves of the CNTs bridges

In order to examine the transport properties of the CNTs bridges across the trench, Fig. 6 shows their I–V characteristics for both as-deposited and annealed (RTA (rapid thermal annealing) treatment at 760 °C) patterns. It indicates metallic properties at lower applied voltages with resistance of about 3×10^{13} and 5×10^{11} ohm for the as-deposited and annealed bridges, respectively. However, it shows in overall a nonlinear I–V relations, signifying non-ohmic contact between bamboo-like MWNTs and Co-catalyst on a:Si. This is in agreement with the proposed statement that the bridges may behave an intramolecular junction (a metal–semiconductor junction) due to defects of the bending parts and cause nonlinear electron transport characteristics [10].

4. Conclusions

In this paper, we have successfully and selectively synthesized the horizontally grown CNT bridges on the Ni-coated parts of a patterned silicon wafer by using MPCVD. The CNTs mainly consist of bamboo-like MWNTs with discrete catalysts split from one original

catalyst particle in the tube. The horizontally-oriented MWNTs are believed to result from the flow restrictions of Si_3N_4 layers and the proper tube number density to minimize the mutual restrictions between the neighboring tubes. The possible reason for forming bamboo-like MWNTs may be the presence of the residual nitrogen on specimen from electroless catalyst deposition. The I–V results indicate in overall a nonlinear I–V relations, signifying non-ohmic contact between bamboo-like MWNTs and Ni-catalyst on a:Si and the resistance of the as-deposited MWNTs can be greatly reduced by subjecting to 760 °C annealing under nitrogen atmosphere.

Acknowledgement

References

[1] Fischer E. John, Johnson T. Alan, Curr. Opin. Solid State Mater. Sci. 4 (1999) 28.
[2] M. Buongiorno Nardelli, J.-L. Fattebert, D. Orlikowski, C. Roland, Q. Zhao, J. Bernholc, Carbon 38 (2000) 1703.
[3] H.R. Astorga, D. Mendoza, Opt. Mater. 27 (2005) 1228.
[4] H.J. Qi, K.B.K. Teo, K.K.S. Lau, M.C. Boycea, W.I. Milne, J. Robertson, K.K. Gleason, J. Mech. Phys. Solids 51 (2003) 2213.
[5] Ph. Lambin, V. Meunier, L. Henrard, A.A. Lucas, Carbon 38 (2000) 1713.
[6] Tokio Yamabe, Masahiro Imade, Motoki Tanaka, Thohru Sato, Synth. Met. 117 (2001) 61.
[7] M.S. Fuhrer, J. Nygrd, L. Shih, M. Forero, Young-Gui Yoon, M.S.C. Mazzoni, Hyoung Joon Choi, Jisoon Ihm, Steven G. Louie, A. Zettl, Paul L. McEuen, Science 288 (2000) 494.
[8] Alain Rochefort, Massimiliano Di Ventra, Phaedon Avouris, Appl. Phys. Lett. 78 (2001) 2521.
[9] Sander J. Tans, Alwin R.M. Verschueren, Cees Dekker, Nature 393 (1998) 49.
[10] Young-Soo Han, Jin-Koog Shin, Sung-Tae Kim, J. Appl. Phys. 90 (2001) 5731.
[11] Chao Hsun Lin, Hui Lin Chang, Chih Ming Hsu, An Ya Lo, Cheng Tzu Kuo, Diamond Relat. Mater. 12 (2003) 1851.
[12] Chih Ming Hsu, Chao Hsun Lin, Hui Lin Chang, Cheng Tzu Kuo, Thin Solid Films 420–421 (2002) 225.
[13] N.R. Franklin, H. Dai, Adv. Mater. 12 (2000) 890.
[14] Y. Zhang, A. Chang, J. Cao, Q. Wang, W. Kim, Y. Li, N. Morris, E. Yenilmez, J. Kong, H. Dai, Appl. Phys. Lett. 79 (2001) 3155.
[15] C. Bower, W. Zhu, S. Jin, O. Zhou, Appl. Phys. Lett. 77 (2000) 830.
[16] S.H. Tsai, C.W. Chao, C.L. Lee, H.C. Shih, Appl. Phys. Lett. 74 (1999) 3462.